Parametric and nonparametric regression models in study of the length of hydraulic jump after a multi-segment sharp-crested V-notch weir

Hamid Saadatnejadgharahassanlou, Rasoul Ilkhanipour Zeynali,
Babak Vaheddoost and Amin Gharehbaghi

ABSTRACT

A multi-segment sharp-crested V-notch weir (SCVW) was used both theoretically and experimentally in this study to evaluate the length of the hydraulic jump at the downstream of the weir. For this aim, a SCVW with three triangular segments at different tail-water depths (tailgate angles), and ten different discharges at a steady flow condition were investigated. Then, the most effective parameters on the length of the hydraulic jump are defined and several parametric and nonparametric regression models, namely multi-linear regression (MLR), additive non-linear regression (ANLR), multiplicative non-linear regression (MNLR), and generalized regression neural network (GRNN) models are compared with two semi-empirical regression models from the literature. The results indicate that the GRNN model is the best model among the selected models. These results are also linked to the nature of the hydraulic jump and the turbulent behavior of the phenomenon, which masks the experimental results with outliers.

Key words | experimental model, length of hydraulic jump, multi-segment sharp crested V-notch weir, open channel flow, parametric and nonparametric model

Hamid Saadatnejadgharahassanlou
Ahar Branch, Civil Engineering Department,
Islamic Azad University,
Tabriz, East Azerbaijan,
Iran

Rasoul Ilkhanipour Zeynali
Water Engineering Department,
Urmia University,
Urmia, West Azerbaijan,
Iran

Babak Vaheddoost (corresponding author)
Faculty of Engineering and Natural Sciences,
Department of Civil Engineering,
Bursa Technical University,
Bursa,
Turkey
E-mail: *babak.vaheddoost@btu.edu.tr*

Amin Gharehbaghi
Department of Civil Engineering,
Dokuz Eylul University,
Tinaztepe Campus, 13 Box 35160, Izmir,
Turkey

NOMENCLATURE

B	Channel width (m);
Fr_1	Approach Froude number [–];
Fr_2	Froude number after hydraulic jump [–];
L	Crest width (m);
L_j	Length of the hydraulic jump (m);
L_j/B	Relative length of the hydraulic jumps [–];
P_1	Crest height (m);
P_2	Height of triangular section (m);
P_3	Weir height (m);
Q	Discharge (lps);
R	Correlation coefficient [–];
R^2	Determination coefficient [–];
Re_1	Incoming Reynolds number [–];
Re_2	Reynolds number after hydraulic jumps [–];
S_0	Slope of main channel bed [–];
β	Intercept in MLR and ANLR;
C_i and ξ_i	Coefficients assigned for ANLR and MNLR;
n	Number of independent variables;
N	Number of data set;
y_i	Estimated ith value for the hydraulic jump;
μ_y	Average of the estimated values for the hydraulic jump;
σ_y	Standard deviation of the estimated values;
g	Acceleration due to gravity (m/s^2);
h	Water head over the crest of weirs (mm);
n	Roughness of the main channel (s/m$^{1/3}$);
y_1	Depth of flow before the hydraulic jumps (mm);
y_2	Depth of flow after the hydraulic jumps (mm);

doi: 10.2166/ws.2019.198

y_c	Critical depth in open channel (mm);
ε	Roughness of the surface ($s/m^{1/3}$);
η	Efficiency of hydraulic jumps [–];
ϕ	Tailgate angles (degree);
μ	Dynamic viscosity of the fluid ($kg/s \cdot m$);
v_1	Mean velocity of flow before hydraulic jumps (m/s);
v_2	Mean velocity of flow after hydraulic jumps (m/s);
ρ	Density of the water (kg/m^3);
σ	Surface tension (N/m);
θ	Vertex angle (degree);
α_i	Constants in MLR and ANLR;
x_i	ith dependent variable in MLR, ANLR and MNLR;
b	Constant in MNLR;
x_i	Observed ith value for the hydraulic jump;
μ_x	Average of the observed values;
σ_x	Standard deviation of the observed values.

INTRODUCTION

The hydraulic jump is a natural phenomenon in which the entrained bubbles are advected into regions, collisions, and coalescence leading to larger air entities that are driven towards the free surface together with the combination of buoyancy and turbulent advection (Chanson 2007).

Several studies have been carried out in order to estimate the length of a hydraulic jump in different conditions (e.g. Vatankhah & Kouchakzadeh 2008; Rashwan 2013; Ahmed et al. 2014). For instance, Gupta et al. (2013) made an effort similar to the previous studies in order to obtain a semi-empirical model with optimized coefficients for defining the length of a hydraulic jump in horizontal channels regarding a rectangular cross-section as:

$$\frac{L_j}{y_1} = 4769.10\left(\frac{Fr_1^{2.10}}{Re_1}\right) + 25.064 \quad (1)$$

where the L_j is calculated using the approach Reynolds number (Re_1), approach depth (y_1), and Froude number (Fr_1).

Silvester (1965) also studied the length of the hydraulic jump in rectangular channels and introduced a dimensionless L_j/y_1 equation as:

$$\frac{L_j}{y_1} = 9.75(Fr_1 - 1)^{1.01} \quad (2)$$

while due to the adequacy and applicability of the diagrams suggested by Bradley & Peterka (1957), Equations (1) and (2) were not widely used in practice. The United States Bureau of Reclamation (USBR 2016) has also introduced several equations for calculating the length of the hydraulic jump in stilling basins based on the length and the existence of any limiting wall of the stilling basin. Similarly, Hager (1992a, 1992b) and Wang & Chanson (2015) also proposed empirical laws related to the dimensionless jump length and the Froude number. In addition to the physical experiments, analytical development of jump roller length was reported by Valiani (1997), which became a point of interest for other researchers as well.

After the development of computers and fast calculating techniques, numerical models had a breakthrough and several techniques were developed in computational fluid dynamics (e.g. Gharehbaghi 2016, 2017; Gharehbaghi et al. 2017). The artificial neural network (ANN) is one of the evolutionary optimization techniques, which is used in many branches of science. Many researchers have used this technique in practice (e.g. Safari et al. 2016; Vaheddoost et al. 2016; Mehdizadeh et al. 2018; Valero & Bung 2018). For instance, Omid et al. (2005) developed an ANN approach for modeling the hydraulic jumps in rectangular and trapezoidal sections. Naseri & Othman (2012) announced the Levenberg–Marquardt (LM) as a more precise ANN technique to determine the L_j in a rectangular section with a horizontal apron. Houichi et al. (2013) used ANN techniques in the estimation of the length of the hydraulic jump in U-shaped channels. More recently, Safari et al. (2016), Khosravinia et al. (2018), and Azimi et al. (2018) used ANN techniques in open channel hydraulics to evaluate several phenomena like sediment motion and deposition.

In this respect, the aim and scope of this study is to (i) conduct experimental studies to investigate the behavior of the SCVW in open channels and (ii) develop several parametric and nonparametric regression models in comparison with several equations from the literature to define the credibility of physical and statistical approaches in practice.

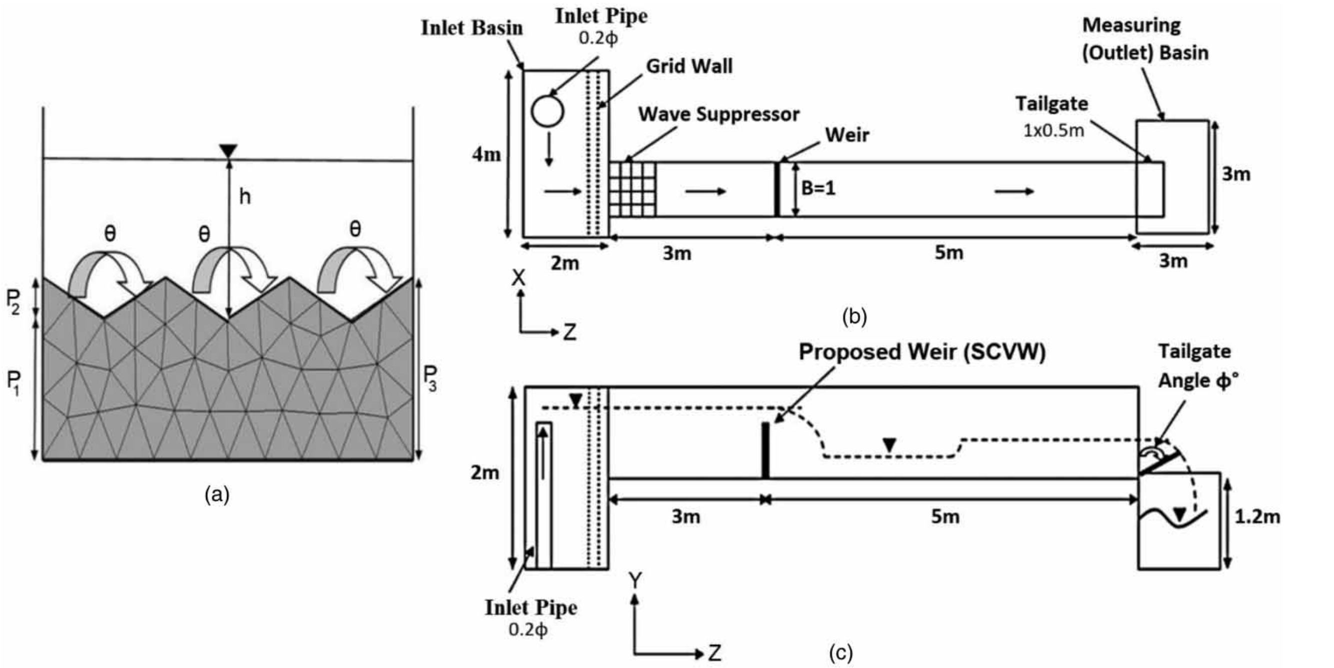

Figure 1 | Sketch view of the SCVW with vertex angle $\theta = 128^{\circ}$ together with (a) the section view, (b) the plan view, and (c) the profile view (*Source*: Saadatnejadgharahassanlou *et al.* 2017).

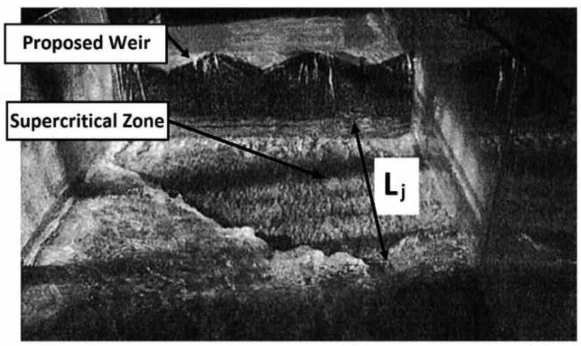

Figure 2 | The experimental measurement and location of L_j in the hydraulic laboratory (Ghaffari *et al.* 2011).

EXPERIMENTAL SET-UP AND MEASURING TECHNIQUES

The experimental parts of the present study were carried out on a multi-segment SCVW in the applied hydraulic laboratory of the Water Engineering Department in Urmia University (Ghaffari *et al.* 2011). The experimental studies were conducted over a model with three segments across a 1 m flume of width L and vertex angle $\theta = 128^{\circ}$, in steady and free overflow conditions. A compound weir criterion of $P_2/h < 1$ was also applied over the model to satisfy the modeling conditions. Thus, h as the water head over the crest of the weir, $P_1 = 0.254$ m as the crest height, $P_2 = 0.08$ m as the height of the triangular cross-section, and $P_3 = 0.334$ m as the weir height are used (data are given in Appendix A).

The characteristics of the model with $\theta = 128^{\circ}$ are given in Figure 1(a). Figure 1(a)–1(c) show the experiment that was conducted with a 3 mm steel plate with sharpened edges and supported by another 5 cm plate to avoid it from bending through overtopping of the flow and was located 3 m from the inlet of the channel at the downstream. Wave suppressors, grid walls, and a tailgate at the outlet were also used respectively to break the large eddies, dissipate the water surface disturbances, and control the water depths at the downstream. The jumps were initiated after the weir, whilst the end of the jump was observed at the point which was determined by the beginning of the jump plus the length of the jump, L_j (Bradley & Peterka 1957; Hager 1992a, 1992b). Figure 2 illustrates the location and length of the skewed hydraulic jump, while Table A1 in Appendix A shows the exact measurements. This length was measured using a ruler with a precision of ± 5 mm. At the end of the jump, macro-scale vortices developed into the jump roller and interacted with the free surface, leading to air entrainment, splashes, and droplet formation in the two-phase flow region (Chanson & Brattberg 2000; Chanson 2007; Murzyn & Chanson 2009). The air entrainment occurred in the form of air bubbles and air packets entrapped at the impingement of the upstream jet flow with the roller (Chanson 2007). Based on experimental observations and Froude number, two types of hydraulic jump were formed. First was an undular jump (N_{Fr}: 1–3), which was not well formed, together with turbulence. The second one was a weak jump (N_{Fr}: 3–6), which occurred when the water velocity was low. It is important to mention that in this study, according to experimental observation, none of the formed hydraulic jumps were submerged.

Dimensional analysis

Collected data were analyzed to assess the effective variables on the flow and hydraulic jump phenomenon in SCVWs. In this respect, this phenomenon can be expressed as:

$$f(y_1, y_2, B, v_1, v_2, L_j, \rho, n, \eta, \varepsilon, g, \mu, S_0, \sigma, \theta) = 0 \tag{3}$$

Although Borghei *et al.* (1999) stated that the effects of S_0, n, σ, ε, and μ on L_j can be negligible since surface tension is very small in nappe heights (i.e. the minimum nappe height over the weir was taken as 20 mm), in the experimental study, the effect of μ was employed to investigate the effect of Re_1 and Re_2 on the results.

Thereby, the dimensionless groups were obtained as:

$$f_1(\Pi_1, \Pi_2, \Pi_3, \Pi_4, \Pi_5, \Pi_6, \Pi_7) = 0 \tag{4}$$

By using the Buckingham π-theorem and applying the properties of dimensional analysis, non-dimensional equations can be obtained as $\Pi_1 = L_j/y_1$, $\Pi_2 = v_1^2/gy_1$, $\Pi_3 = v_2^2/gy_2$, $\Pi_4 = \rho v_1 y_1/\mu$, $\Pi_5 = \rho v_2 y_2/\mu$, $\Pi_6 = y_2/B$, $\Pi_7 = \theta$.

These equations can be inserted in Equation (4) and rewritten as:

$$\frac{L_j}{y_1} = f_3\left(Fr_1, Fr_2, Re_1, Re_2, \frac{y_2}{B}, \theta\right) \tag{5}$$

where y_1 and y_2 are sequent depths used in the calculations. Equation (5) is the motivation in selection of the variables and modeling criteria in the remaining parts of the study.

Table 1 | Statistical properties of normalized data used in this study

Variable	Mean (m)	Standard deviation (m)	Coefficient of variation (–)	Skewness (–)	Kurtosis (–)
L_j	0.15	0.28	1.89	1.99	3.19
Fr_1	0.26	0.27	1.04	1.00	0.07
Re_1	0.40	0.31	0.76	0.76	−0.73
Y_1	0.36	0.24	0.67	0.84	0.04

Variable selection and data analysis

Based on the previous studies (e.g. Silvester 1965; Gupta *et al.* 2013) and the dimensional analysis, Fr_2, Re_2, θ, ϕ, and y_2/B are negligible and Equation (5) can be rewritten as

$$\frac{L_j}{y_1} = f_3(Fr_1, Re_1) \tag{6}$$

Since the aim of the study is to develop models to compare with equations obtained by Gupta *et al.* (2013) and Silvester (1965), in the rest of the study Equation (6) and its variables are used to study the length of the hydraulic jump, L_j.

A data set of 42 observations, recorded for L_j, Fr_1, Re_1, and y_1, were used (see Table A1 in Appendix A). To avoid misinterpretation, providing iso-dimensionality on both sides of the equation, and minimizing the precision, all data sets were normalized (Table 1). Figure 3(a) shows the nonlinear nature of the relationship between Fr_1 and y_1. Similarly, in Figure 3(b) and 3(c) the relationship between Re_1 is given compared with y_1 and Fr_1 respectively. In addition, Figure 3(d)–3(f) show the relationship between L_j compared with y_1, Fr_1, and Re_1 respectively. In Figure 3(d), results are very similar to those obtained for Figure 3(a), and the relationship of L_j with Fr_1 and Re_1 in Figure 3(e)–3(f) seems quite complicated. Based on the results of Figure 3, it is obvious that a high precision in modeling would be inevitable.

It is noteworthy that the zero values associated with the L_j could be explained when the hydraulic jump is not formed. Therefore, the selected models also have to consider whether the jump is formed or not. As seen in Table 1, deviations from means caused a lot of variations. It is obvious that the L_j has the most unstable behavior by means of the highest coefficients of variation and skewness. Particularly, in Figure 3(d)–3(f) a lot of deviations occurred when L_j is expressed by y_1, Fr_1, or Re_1. In Figure 3, the dashed line

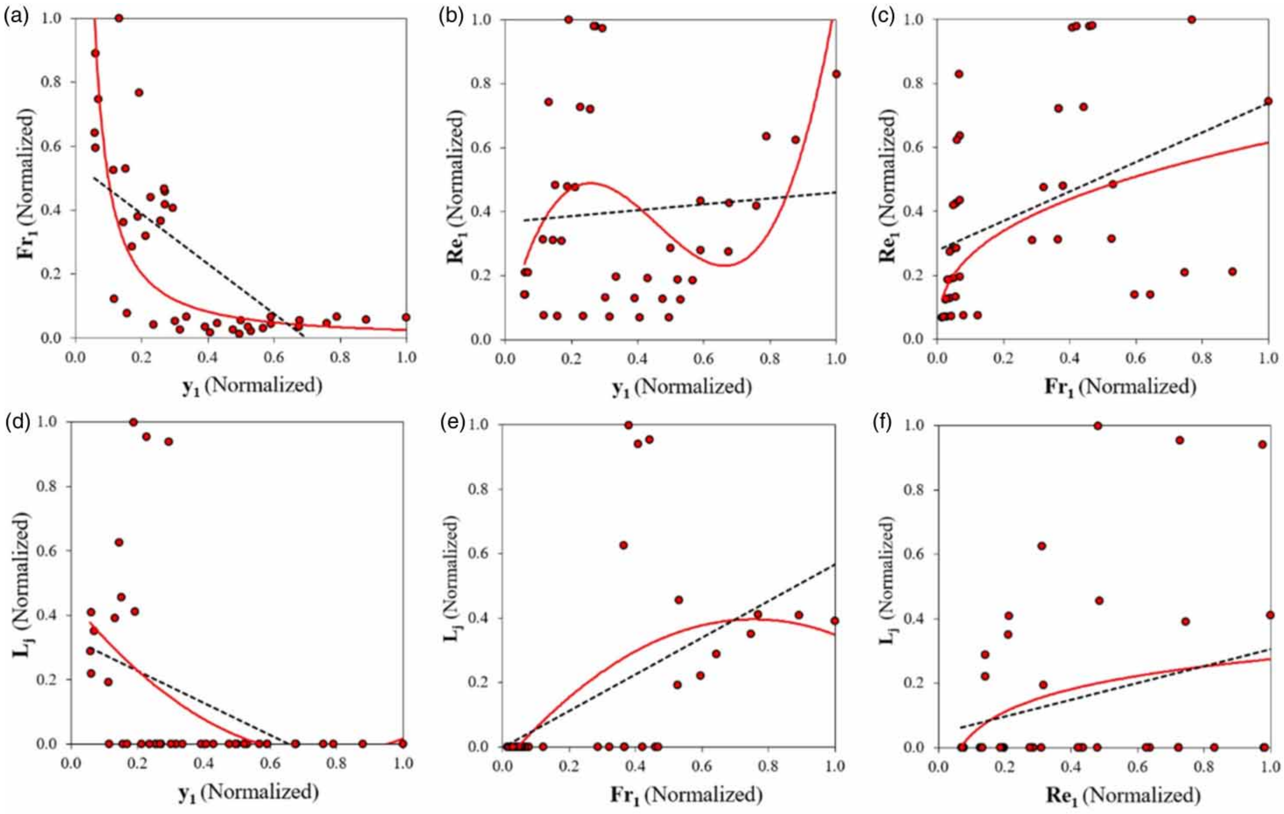

Figure 3 | Scatter-plot of relation between normalized variables including (a) Fr_1 versus y_1, (b) Re_1 versus y_1, (c) Re_1 versus Fr_1, (d) L_j versus y_1, (e) L_j versus Fr_1, and (f) L_j versus Re_1. Please refer to the online version of this paper to see this figure in color: http://dx.doi.org/10.2166/ws.2019.198.

(in black) as the linear relation of the data versus the continuous line (in red) as the second-degree polynomial fit of the data show several similarities, whilst the dissimilarities between linear and non-linear lines are too coarse to be detailed easily. Since non-excludable outliers were included (i.e. data related to hydraulic jump in Figure 3(d)–3(f); Table A1), outlier-resistant nonparametric approaches are also used in the analysis to deal with the rank of the data set.

MODELING

In this study, several parametric regression models, namely multi-linear regression (MLR), additive non-linear regression (ANLR), and multiplicative non-linear regression (MNLR) models are used together with the equations suggested by Silvester (1965) and Gupta *et al.* (2013). The nonparametric generalized regression neural network (GRNN) was also used along with the selected parametric models due to its non-linear outlier-resistance nature in function approximation. Models were developed to estimate the length of hydraulic jump based on Re_1, Fr_1, and y_1 as:

$$L_j = f(Fr_1, Re_1, y_1) \quad (7)$$

First, a set of 33 randomly selected observations (80% of the data) is used in model calibration and model approximation. Then, the remaining sets of the data with nine sets of observations (20%) for each variable, namely test data, is used in evaluation of the models. In this respect, several criteria are used to evaluate each model.

Multi-linear regression (MLR)

The goal in a linear regression analysis is to determine coefficients (α_i) and an intercept (β) to expose the linear relationship between input variables (x_i), and the output variable (y) such that:

$$y = \sum_{i=1}^{n} \alpha_i x_i + \beta \quad (8)$$

Coefficients and the intercept for linear regression are obtained by minimizing the difference between the observed values and model outputs using the ordinary least squares method.

Non-linear regression (NLR)

Herein, an additive and a multiplicative combination of variables are used in modeling as Vaheddoost et al. (2016) introduced them as useful key models in defining non-linearity in water resource studies. These models respectively for additive (ANLR) and multiplicative (MNLR) regression are:

$$y = \sum_{i=1}^{n} \alpha_i x_i^{c_i} + \beta \tag{9}$$

$$y = b \prod_{i=1}^{n} x_i^{\xi_i} \tag{10}$$

In this study, a Levenberg–Marquardt (LM) algorithm (Moré 1978) is used in coefficient estimation.

Generalized regression neural network (GRNN)

GRNN is a four-layered ANN model of a one-pass learning algorithm with a highly parallel structure used when the assumption of linearity is not justified (Specht 1991). The first layer contains the input vectors of independent variables, whilst the second one is a summation layer, which has two neurons called S-summation and D-summation. The third layer covers the output vector obtained for each input vector, which can be expressed as:

$$y_i(\boldsymbol{x}) = \frac{\sum_{i=1}^{p} \omega_i e^{-D(x,x_i)}}{\sum_{i=1}^{p} e^{-D(x,x_i)}} \tag{11}$$

Performance evaluation criteria

Several performance criteria are used to compare models with each other. For this aim, determination coefficient (R^2), Lin's concordance correlation coefficient (CC), performance index (PI) and root mean square percentage error ($RMSPE$) are considered and respectively defined as:

$$R^2 = \left(\frac{\sum_{i=1}^{N} (x_i - \mu_x)(y_i - \mu_y)}{N\sigma_x \sigma_y} \right)^2 \tag{12}$$

$$CC = \frac{2\rho_{xy}\sigma_x\sigma_y}{\sigma_x^2 + \sigma_y^2 + (\mu_x - \mu_y)^2} \tag{13}$$

$$PI = \frac{1}{N} \sum_{i=1}^{N} \frac{y_i}{x_i} \tag{14}$$

$$RMSPE = \frac{1}{\mu_x} \sqrt{\frac{\sum_{i=1}^{N} (x_i - y_i)^2}{N}} \times 100 \tag{15}$$

Also, mean absolute error (MAE) is used in the monitoring of GRNN model calibration as:

$$MAE = \frac{\sum_{i=1}^{N} |y_i - x_i|}{N} \tag{16}$$

where N is the number of data sets.

Model grading

For this aim, the method suggested by Vaheddoost et al. (2016) is used. Hence, success grade (SG) and failure grade (FG) of the performance criteria are defined as:

$$SG(R^2)_i = \frac{R_i^2}{R_{\max}^2} \times 10 \tag{17}$$

$$SG(CC)_i = \left| \frac{CC_i}{CC_{\max}} \right| \times 10 \tag{18}$$

$$FG(PI)_i = \left(\frac{|1 - PI|_{\min}}{|1 - PI|_i} \times 10 \right) - 10 \tag{19}$$

$$FG(RMSPE)_i = \left(\frac{RMSPE_{\min}}{RMSPE_i} \times 10 \right) - 10 \tag{20}$$

The total grade of each model is obtained by adding up the SGs and FGs of each model individually, which can differ between +20 and −20.

RESULTS AND DISCUSSION

Results of the experimental studies

Based on the laboratory experiments, when using SCVWs, by increasing Fr_1 and Re_1, the values of L_j would increase. Moreover, the current weir causes formation of additional blades in water jets at the downstream. Hence, by collision of the falling water jets at the downstream, L_j decreases, noticeably. As a result, by decreasing L_j, the length of the stilling basin, effects of the scour, and erosion phenomena in downstream channels will reduce. This advantage induces a decrease in the construction costs of the stilling basin. The interested reader may also refer to Saadatnejadgharahassanlou *et al.* (2017) for more details about the experimental study.

Evaluation of models in train data (model fitting)

MLR model

The best MLR model was obtained as:

$$L_j = 0.507\,Fr_1 \tag{21}$$

in which the normalized length of the hydraulic jump is assumed to be about 50% of the normalized Fr_1 with an R^2 of 0.36.

NLR model

The best ANLR and MNLR models are also obtained. Since the best ANLR model, as:

$$L_j = 1923.66\,y_1^{0.001} + 11.04\,Fr_1^{0.099} - 1932.16\,Re_1^{0.0004} \tag{22}$$

gives an R^2 of 0.27 and estimates negative results for the length of the hydraulic jump, it was excluded from the analysis.

On the other hand, the best MNLR model with R^2 of 0.45 showed more dependable results using:

$$L_j = \frac{92254949.31(y_1^{10.32})(Fr_1^{8.06})}{Re_1^{6.87}} \tag{23}$$

GRNN model

The GRNN model is also developed by a set of 12 different spread parameters. Figure 4 shows the results of different spread parameters on model results. The *PI* criterion gradually increased through different spread parameters from 1 to 0.2 and decreased afterward. Based on the results of the *PI* and *MAE*, a model with spread parameter 0.2 could be selected in GRNN calibration.

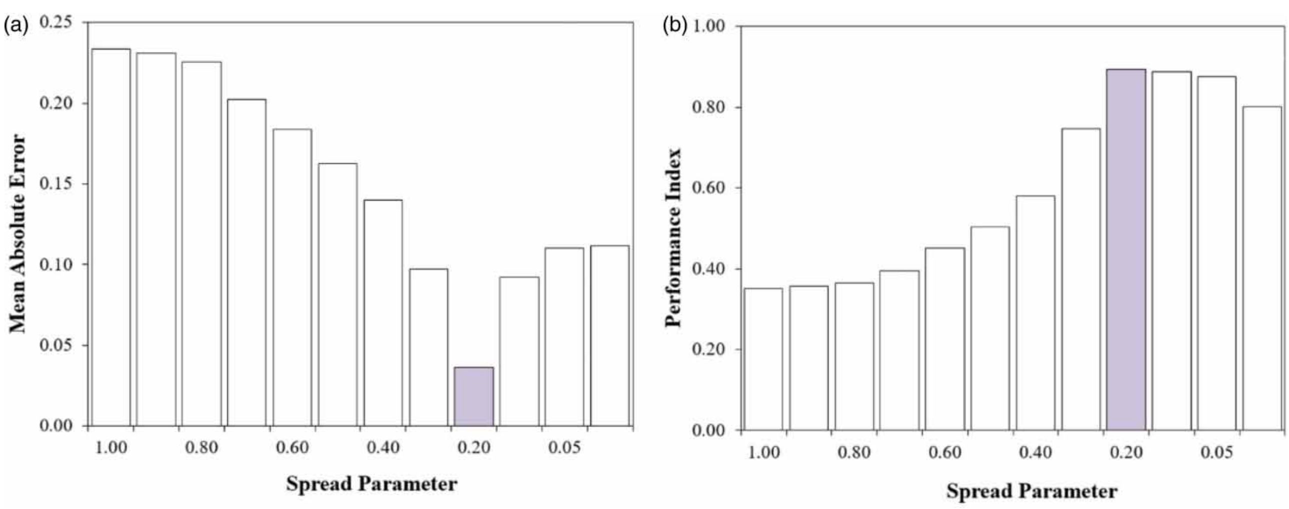

Figure 4 | Model calibration for GRNN by means of the (a) *MAE* and (b) *PI* criterion.

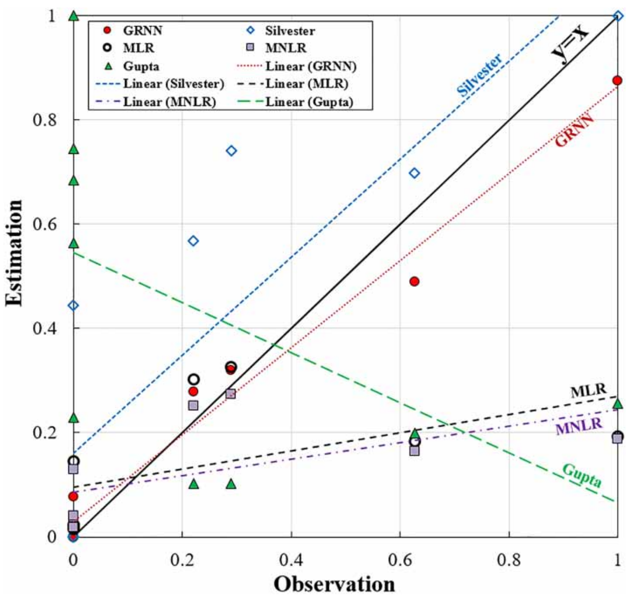

Figure 5 | Scatter-plot of all models in test.

Evaluation of models in test data

Results of all models including MLR, MNLR, GRNN, Silvester (1965) and Gupta *et al.* (2013) were compared using a scatter-plot (Figure 5), R^2, *CC*, *PI*, *RMSPE*, and the total grades obtained by Equations (17)–(20) (Table 2).

According to Figure 5 and Table 2, GRNN is the best model, whilst the results obtained by the Silvester (1965) equation are the second best. Figure 5 also shows that the GRNN and the Silvester (1965) models are eligible, while the results obtained by the other models have significant bias in estimation. On the other hand, the equation suggested by Gupta *et al.* (2013) has the worst results. Since the experiments are conducted on a SCVW, it is not obvious if the type of weir could cause deviation from the results obtained by Silvester (1965) or Gupta *et al.* (2013). Thereby, along with the data analysis given in Table 1 and Figures 3–5, the obtained results indicate strong deviations that mislead the parametric modeling in practice. The moments of the distribution and the parametric approaches seem to be less desirable in this approach. Due to the high accuracy and existence of outliers, nonparametric GRNN shows the best performance. Its superior performance can also be related to the higher number of individually taken input variables in a one-way pass classification that is lumped in parametric regression models. Thereby, along with the results of Specht (1991), it is obvious that the justification of linearity or non-linearity in the parametric approach is vital. In addition, GRNN is bounded to the minimum and maximum values of the observation data, which could not be achieved by the ANLR model when estimating negative values.

It is concluded that the GRNN as the representative of the nonparametric models is superior in comparison to those parametric approaches used in this study. Obviously, outliers associated with the hydraulic jump can only be carried out based on the associated rank of each observation in the data set (Table 1 and Table A1). The idea of the parametric reduction in this sense may need an update due to the high uncertainty associated with phenomena like hydraulic jump.

CONCLUSIONS

In this study, a multi-segment sharp-crested V-notch weir, termed SCVW, has been used. Extensive laboratory experiments were conducted to measure the length of hydraulic jump at the downstream of the SCVW. It was observed that by increasing the approach *Fr* and *Re* the length of the hydraulic jump would increase and vice versa. As a

Table 2 | Results of all models in test data set and related grades

Model	R^2	SG (R^2)	*CC*	SG (*CC*)	*PI*	FG (*PI*)	*RMSPE* (%)	FG (*RMSPE*)	Total grade
MLR	0.25	+2.55	0.29	+3.24	0.75	−9.76	131.59	−7.75	−11.71
MNLR	0.31	+3.16	0.27	+3.00	0.63	−9.83	132.80	−7.77	−11.44
GRNN	0.98	+10.00	0.88	+10.00	1.01	−0.00	29.62	−0.00	+20.00
Silvester	0.73	+7.48	0.83	+9.34	1.81	−9.92	101.94	−7.09	−0.20
Gupta	0.28	+2.84	−0.53	+5.93	0.35	−9.91	250.35	−8.82	−9.94

result, by decreasing L_j, the length of the stilling basin, effects of the scour, and the erosion phenomena at the downstream of the channels will decrease, which also decreases the construction costs of the stilling basin.

In addition, three types of parametric regression models, (i.e. MLR, ANLR, and MNLR), two models from the literature (i.e. Silvester 1965; Gupta *et al.* 2013), and a non-parametric regression model (i.e. GRNN) are used in modeling. Evaluation of the models was conducted in two stages, training and testing. For this aim several performance criteria, namely R^2, *CC*, *PI*, *RMSPE*, *MAE*, and total grade are used. The results indicate that the GRNN model with a nonparametric regression approach is the superior model whilst the Silvester (1965) model is the second best. It is concluded that the high uncertainty and skewness associated with the length of L_j, together with the presence of outliers, is better expressed in nonparametric regression, i.e. GRNN. It is obvious that the rank of the data in each allocated set is more dependable than the moments of the distribution.

ACKNOWLEDGEMENT

The authors appreciate the cooperation of Urmia University in conducting the experiments.

CONFLICT OF INTEREST

None.

SUPPLEMENTARY MATERIAL

The Supplementary Material for this paper is available online at https://dx.doi.org/10.2166/ws.2019.198.

REFERENCES

Ahmed, H. M. A., El Gendy, M., Mirdan, A. M. H., Ali, A. A. M. & Haleem, F. S. F. A. 2014 Effect of corrugated beds on characteristics of submerged hydraulic jump. *Ain Shams Engineering Journal* **5** (4), 1033–1042.

Azimi, H., Bonakdari, H., Ebtehaj, I., Gharabaghi, B. & Khoshbin, F. 2018 Evolutionary design of generalized group method of data handling-type neural network for estimating the hydraulic jump roller length. *Acta Mechanica* **229** (3), 1197–1214.

Borghei, S. M., Jalili, M. R. & Ghodsian, M. 1999 Discharge coefficient for sharp-crested side weir in subcritical flow. *Journal of Hydraulic Engineering* **125** (10), 1051–1056.

Bradley, J. N. & Peterka, A. J. 1957 The hydraulic design of stilling basins: hydraulic jumps on a horizontal apron (basin I). *Journal of the Hydraulics Division* **83** (5), 1–24.

Chanson, H. 2007 Bubbly flow structure in hydraulic jump. *European Journal of Mechanics – B/Fluids* **26** (3), 367–384.

Chanson, H. & Brattberg, T. 2000 Experimental study of the air–water shear flow in a hydraulic jump. *International Journal of Multiphase Flow* **26** (4), 583–607.

Ghaffari, M., Ahanyar, A. & Hasanzadeh, M. 2011 *Analysis of Sharp Crested V-Notch Weirs in Comparison with Linear Weir of the Same Height*. BSc, Elective Graduation Project, Department of Water Engineering, Faculty of Agriculture, Urmia University, Urmia, Iran.

Gharehbaghi, A. 2016 Explicit and implicit forms of differential quadrature method for advection–diffusion equation with variable coefficients in semi-infinite domain. *Journal of Hydrology* **541**, 935–940.

Gharehbaghi, A. 2017 Third- and fifth-order finite volume schemes for advection–diffusion equation with variable coefficients in semi-infinite domain. *Water and Environment Journal* **31** (2), 184–193.

Gharehbaghi, A., Kaya, B. & Saadatnejadgharahassanlou, H. 2017 Two-dimensional bed variation models under non-equilibrium conditions in turbulent streams. *Arabian Journal for Science and Engineering* **42** (3), 999–1011.

Gupta, S. K., Mehta, R. C. & Dwivedi, V. K. 2013 Modeling of relative length and relative energy loss of free hydraulic jump in horizontal prismatic channel. *Procedia Engineering* **51**, 529–537.

Hager, W. H. 1992a Discussion of 'Design procedure for flow over side weirs' by Ali Uymaz and Roger H. Smith (January/February, 1991, Vol. 117, No. 1). *Journal of Irrigation and Drainage Engineering* **118** (2), 340–340.

Hager, W. H. 1992b Discussion of 'Force on slab beneath hydraulic jump' by Javad Farhoudi and Rangaswami Narayanan (January, 1991, Vol. 117, No. 1). *Journal of Irrigation and Drainage Engineering* **118** (4), 666–667.

Houichi, L., Dechemi, N., Heddam, S. & Achour, B. 2013 An evaluation of ANN methods for estimating the lengths of hydraulic jumps in U-shaped channel. *Journal of Hydroinformatics* **15** (1), 147–154.

Khosravinia, P., Sanikhani, H. & Abdi, C. 2018 Application of soft computing techniques to predict of hydraulic jump length on rough beds. *Journal of Rehabilitation in Civil Engineering* **6** (2), 148–165.

Mehdizadeh, S., Behmanesh, J. & Khalili, K. 2018 New approaches for estimation of monthly rainfall based on GEP-ARCH and

ANN-ARCH hybrid models. *Water Resources Management* **32** (2), 527–545.
Moré, J. J. 1978 The Levenberg–Marquardt algorithm: implementation and theory. In: *Numerical Analysis* (G.A. Watson, ed.), Springer, Berlin and Heidelberg, pp. 105–116.
Murzyn, F. & Chanson, H. 2009 Two-phase gas–liquid flow properties in the hydraulic jump: review and perspectives. In: *Multiphase Flow Research* (S. Martin & J. R. Williams, eds), Nova Science Publishers, New York, USA, pp. 497–542.
Naseri, M. & Othman, F. 2012 Determination of the length of hydraulic jumps using artificial neural networks. *Advances in Engineering Software* **48**, 27–31.
Omid, M. H., Omid, M. & Esmaeeli Varaki, M. 2005 Modelling hydraulic jumps with artificial neural networks. *Proceedings of the Institution of Civil Engineers – Water Management* **158** (2), 65–70.
Rashwan, I. M. H. 2013 Analytical solution to problems of hydraulic jump in horizontal triangular channels. *Ain Shams Engineering Journal* **4** (3), 365–368.
Saadatnejadgharahassanlou, H., Gharehbaghi, A., Mehdizadeh, S., Kaya, B. & Behmanesh, J. 2017 Experimental investigation of discharge coefficient over novel kind of sharp-crested V-notch weir. *Flow Measurement and Instrumentation* **54**, 236–242.
Safari, M. J. S., Aksoy, H. & Mohammadi, M. 2016 Artificial neural network and regression models for flow velocity at sediment incipient deposition. *Journal of Hydrology* **541**, 1420–1429.
Silvester, R. 1965 Theory and experiment on the hydraulic jump. In: *Proceedings of the 2nd Australasian Conference on Hydraulics and Fluid Mechanics*, University of Auckland, New Zealand, pp. A25–A39.
Specht, D. F. 1991 A general regression neural network. *IEEE T. Neural Networks* **2** (6), 568–576.
United States Bureau of Reclamation (USBR) 2016 *Design of Basins*. https://www.usbr.gov/ (accessed January 2016).
Vaheddoost, B., Aksoy, H. & Abghari, H. 2016 Prediction of water level using monthly lagged data in lake Urmia, Iran. *Water Resources Management* **30** (13), 4951–4967.
Valero, D. & Bung, D. B. 2018 Artificial neural networks and pattern recognition for air–water flow velocity estimation using a single-tip optical fibre probe. *Journal of Hydro-Environment Research* **19**, 150–159.
Valiani, A. 1997 Linear and angular momentum conservation in hydraulic jump. *Journal of Hydraulic Research* **35** (3), 323–354.
Vatankhah, A. R. & Kouchakzadeh, S. 2008 Discussion of 'Solution of specific energy and specific force equations' by Amlan Das. *Journal of Irrigation and Drainage Engineering* **134** (6), 880–882.
Wang, H. & Chanson, H. 2015 Experimental study of turbulent fluctuations in hydraulic jumps. *Journal of Hydraulic Engineering* **141** (7), 04015010.

First received 5 July 2019; accepted in revised form 8 December 2019. Available online 30 December 2019